

Beware the Pitfalls of CO₂ Freezing Prediction

TIM EGGEMAN
STEVE CHAFIN
 RIVER CITY ENGINEERING, INC.

Carbon dioxide freezing in a cryogenic system can result in plugging and other operational problems. This article offers insights into the CO₂ freezing phenomenon.

CRYOGENIC PROCESSES ARE USED IN natural gas plants, petroleum refineries, ethylene plants and elsewhere in the process industries to recover and purify products that would normally be gaseous at ambient temperature and pressure. Carbon dioxide can freeze at the low temperatures encountered in cryogenic plants, leading to plugged equipment and other operating problems. Accurate and reliable predictions of CO₂ freeze points are needed for the design of cryogenic systems to ensure that freeze conditions are avoided. CO₂ freeze-out prevention may dictate the type of cryogenic recovery process utilized, the maximum achievable recovery of products, or the amount of CO₂ recovered from the feed gas.

During the revamp of a cryogenic natural gas plant, several commercial process simulators inaccurately predicted CO₂ freeze points. Table 1 compares commercial simulator predictions with experimental liquid/solid equilibrium (LSE) freeze point data for the methane-CO₂ binary system found in GPA Research Report RR-10 (1). It is evident that the process simulator results do not reliably match the experimental data for even this simple system.

This article reviews existing experimental data and the thermodynamics of solid CO₂ formation in both liquids and vapors, presents calculation methods tailored to equipment commonly encountered

in cryogenic processes, and tests our predictions against the freeze points observed in several commercial-scale cryogenic plants known to be constrained by CO₂ solid formation. While the focus is on CO₂ freeze point predictions for natural gas plant applications, the methodology can be readily extended to other solutes and other applications.

There are two basic modes for formation of solid CO₂. Where the CO₂ content of a liquid exceeds its solubility limit, CO₂ precipitates or crystallizes from the liquid solution, as described by the thermodynamics of liquid/solid equilibria (LSE). Where the CO₂ content of a vapor exceeds the solubility limit, CO₂ is formed by desublimation or frosting, which is described by the thermodynamics of vapor/solid equilibria (VSE).

Table 1. Methane-CO₂ binary freezing comparison (LSE).

Mole Fraction Methane	Mole Fraction CO ₂	Temperature, °F				This Work
		Experimental (1)	Simulator A	Simulator B	Simulator C	
0.9984	0.0016	-226.3	-196.3	-239.2	-236.4	-226.2
0.9975	0.0025	-216.3	-186.9	-229.3	-227.0	-217.3
0.9963	0.0037	-208.7	-178.8	-220.1	-218.1	-209.0
0.9942	0.0058	-199.5	-169.0	-208.8	-207.1	-198.7
0.9907	0.0093	-189.0	-158.1	-195.9	-158.0	-187.2
0.9817	0.0183	-168.0	-140.0	-175.5	-140.0	-168.9
0.9706	0.0294	-153.9	-127.3	-159.9	-160.9	-154.9
0.9415	0.0585	-131.8	-108.1	-135.1	-108.1	-133.1
0.8992	0.1008	-119.0	-92.9	-90.8	-92.9	-116.4
0.8461	0.1539	-105.2	-88.1	-82.1	-88.0	-105.5
0.7950	0.2050	-97.4	-99.4	-83.6	-99.4	-99.5
Maximum Absolute Deviation			30.9	28.2	31.0	2.6

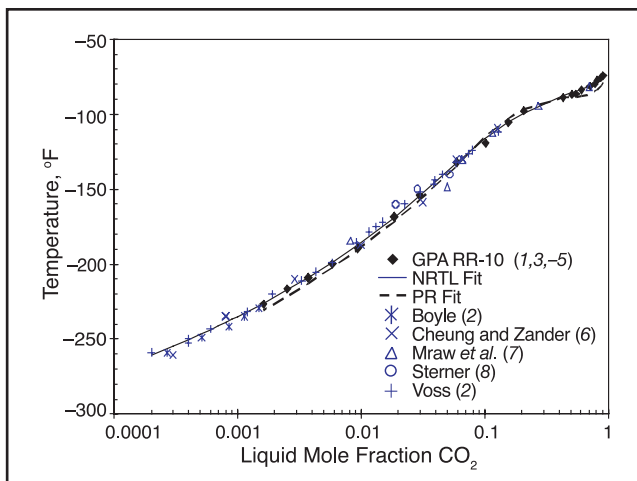


Figure 1. Solubility of CO₂ in liquid methane.

Liquid/solid equilibria

The GPA Research Report RR-10 (1) and Knapp, *et al.* (2) are good resources for many of the original papers containing experimental data for the liquid/solid systems of interest. The data presented in GPA RR-10 are of high quality. The measurements are based on triple point experiments and include records of the system pressure for each experiment, which is needed when correlating with an equation of state.

Figure 1 is a plot of experimental data (1–8) for the solubility of CO₂ in liquid methane. Similar experimental data for the ethane-CO₂ binary system (6, 9, 10), propane-CO₂ binary system (6, 9), methane-ethane-CO₂ ternary system

(9), methane-propane-CO₂ ternary system (11), ethane-propane-CO₂ ternary system (11), and the methane-ethane-propane-CO₂ quaternary system (11) are also available.

The starting point for deriving any phase equilibrium relationship is equating partial fugacities for each component in each phase. Only one meaningful equation results if one makes the normal assumption of a pure CO₂ solid phase. Then one has to decide whether to use an activity coefficient or an equation-of-state approach.

Equation 1 holds at equilibrium when using an activity coefficient model

We chose the Non-Random Two Liquid (NRTL) equation to model the activity coefficient, because it is applicable to multi-component mixtures and is capable of handling the expected level of non-ideality. The binary interaction parameters between methane and CO₂ were regressed using the GPA RR-10 data in Figure 1. The resulting fit agrees well over the entire range. The absolute value of the maximum deviation from the GPA RR-10 data is 2.6°F, a much closer fit than any of the simulator predictions. The absolute value of the maximum deviation from the data sets presented in sources other than GPA RR-10 is 9.4°F, reflecting a higher degree of scatter.

We also regressed NRTL parameters to predict CO₂ freezing of liquid mixtures containing methane, ethane and propane. These four components (CO₂, methane, ethane, propane) were responsible for over 99% of the species present in our original revamp problem; the remaining species were mapped into either methane or propane according to boiling

point. The error caused by this approximation should be quite small, but it does point to some of the limitations of the activity model approach: limited accuracy of predictive modes for generating key interaction parameters through UNIFAC or similar means; difficulties in handling supercritical components via Henry’s law; and the need to generate a large number of non-key interaction parameters in a rational manner.

Switching to an equation-of-state model, Eq. 2 holds at equilibrium.

Any equation of state can be used to calculate the required fugacities; we chose a standard form of the Peng-Robinson equation, since it is widely used to model natural gas processing systems. Binary interaction parameters for all of the non-key pairs were set to their values derived from VLE regressions. (VLE-based interaction parameters can also be used with CO₂ pairs, resulting in surpris-

$$\ln \gamma_{CO_2} x_{CO_2} = \frac{(S_{L,TP} - S_{S,TP})}{R} \left(1 - \frac{T_{TP}}{T}\right) - \frac{[(a_L - a_S) - (b_L - b_S)T]}{R} \left(1 - \frac{T_{TP}}{T}\right) + \frac{(a_L - a_S)}{R} \ln\left(\frac{T}{T_P}\right) - \frac{(b_L - b_S)}{2R} T \left[1 - \left(\frac{T_{TP}}{T}\right)^2\right] \tag{1}$$

$$x_{CO_2} \phi_{CO_2}^L P = P_{CO_2Solid}^{Sat} \phi_{CO_2}^{Sat} \exp\left[\frac{V_{CO_2Solid}}{RT} (P - P_{CO_2Solid}^{Sat})\right] \tag{2}$$

$$z^3 - (1 - B)z^2 + (A - 3B^2 - 2B)z - (AB - B^2 - B^3) = 0 \tag{3}$$

$$y_{CO_2} \phi_{CO_2}^V P = P_{CO_2Solid}^{Sat} \phi_{CO_2}^{Sat} \exp\left[\frac{V_{CO_2Solid}}{RT} (P - P_{CO_2Solid}^{Sat})\right] \tag{4}$$

$$T \leq T_{TP} \tag{5}$$

Equations 1–5.

ing accuracy. We have found, though, slightly better performance when the interaction parameters for the CO₂ pairs are regressed from experimental data.)

Figure 1 compares the fitted Peng-Robinson (PR) model predictions for the CO₂-methane binary system with the experimental data and the NRTL model predictions. The accuracy of the Peng-Robinson model is comparable to that of the NRTL model in the -150°F region, but falls off in other areas. The absolute value of the maximum deviation from the GPA RR-10 data is 6.4°F. We were surprised by the ability of the Peng-Robinson equation of state to accurately model this system given the high degree of non-ideality.

While the equation-of-state approach has the advantage of providing a consistent theoretical framework that is more easily extended to new situations, the details of the numerical procedures required are more complex. For example, when the Peng-Robinson cubic equation of state is used, one needs to find roots of Eq. 3. The resulting compressibility is then inserted into the appropriate fugacity equation and then Eq. 2 is root-solved to find the conditions (*T*, *P* and composition) where solid CO₂ begins to form.

There are up to three real roots for Eq. 3. Analytical solution, via Cardan's Rule, can produce meaningless results, since the required calculations are sensitive to round-off errors (14). We have found that eigenvalue-based methods work well and accurately provide all three roots, whether real or complex (15).

The root-solving algorithm for Eq. 2 should be initialized with a reasonably good guess to avoid problems when computing compressibilities from Eq. 3. Unfortunately, empirical root-discrimination methods for VLE flashes, such as the method by Poling (16), do not always work well with the liquid/solid and vapor/solid flashes considered here. We have found the best way to avoid this pitfall is to use a conservative numerical root-solving method, such as false position, in which the root is always bracketed, and to initialize the calculation with the result of a converged solution to the NRTL formulation.

Vapor/solid equilibria

The experimental data for CO₂ frosting are meager compared to the amount of data available for liquid/solid systems. The Pikaar (17) data set for the CO₂-methane binary is frequently displayed in

the literature, but unfortunately Pikaar's work was never published outside his dissertation. The multi-component triple point data presented in GPA RR-10 is another source of vapor/solid equilibrium data.

Equation-of-state models are best used for modeling vapor/solid systems because they readily provide the required terms. The relevant equilibrium relationships are Eqs. 4 and 5.

Equation 4 is derived by equating partial fugacities; Eq. 5 merely states that the solid must be stable if formed. Quite often, thermodynamic textbooks forget to mention Eq. 5. We have found several cases where solids were predicted from Eq. 4 but the temperature was too high for a stable solid.

As in the liquid/solid case, any equation of state can be used to evaluate the fugacities. We again chose a standard version of the Peng-Robinson equation. This time, due to the lack of data, the binary interaction parameters were defaulted to the values used for VLE calculations. Figure 2 shows that the predictions agree quite well with the experimental methane-CO₂ binary frost point data from Pikaar (17). Compared to the multi-component triple point data in RR-10, the average deviation of the predicted frost point and experimental triple point temperatures at known pressure and composition is 3°F.

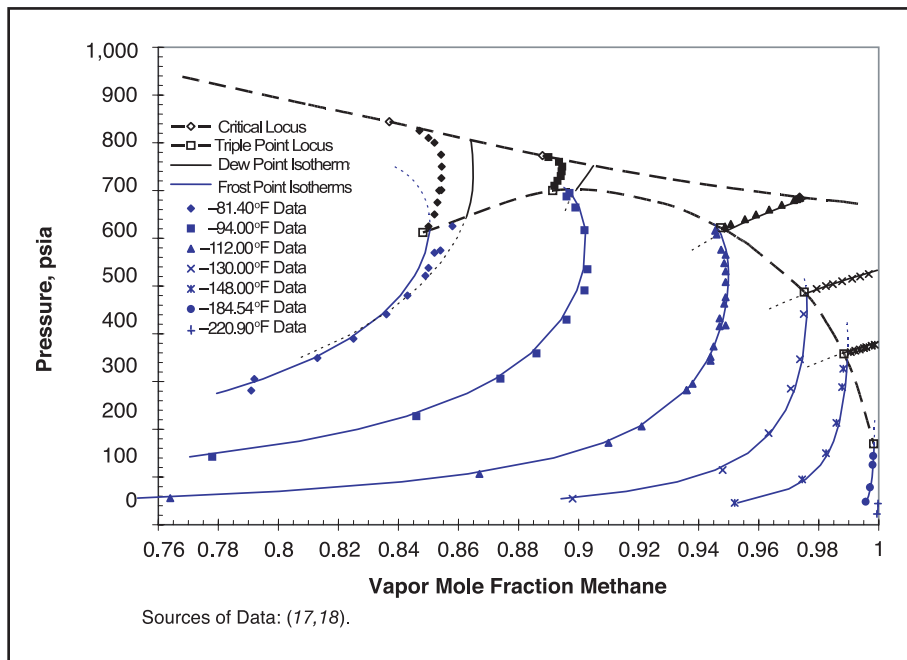
Figure 2 presents extrapolations of the predicted frost point and dew point isotherms. Their intersections define the predicted triple points for this binary system. Our pre-

Nomenclature

<i>A</i> , <i>B</i>	= real constants for Eq. 4 that are constructed from the mixing rules
<i>a_L</i> , <i>b_L</i>	= coefficients for liquid CO ₂ heat capacity, $a_L + b_L T = 3.0477 + 0.0714T$ (13)
<i>a_S</i> , <i>b_S</i>	= coefficients for solid CO ₂ heat capacity, $a_S + b_S T = 5.0745 + 0.0379T$ (13)
<i>P</i>	= system pressure, kPa
<i>P^{Sat}_{CO₂Solid}</i>	= vapor pressure of solid CO ₂ at system temperature, kPa
<i>R</i>	= gas constant = 1.9872 cal/(gmol-K)
<i>S_{L,TP}</i>	= entropy of liquid CO ₂ at the triple point = 27.76 cal/(gmol-K) (12)
<i>S_{S,TP}</i>	= entropy of solid CO ₂ at the triple point = 18.10 cal/(gmol-K) (12)
<i>T</i>	= temperature, K
<i>T_{TP}</i>	= triple point temperature for CO ₂ = 216.55 K (12)
<i>V_{CO₂Solid}</i>	= molar volume of solid CO ₂ , cm ³ /gmol
<i>x_{CO₂}</i>	= mole fraction of CO ₂ in the liquid phase, dimensionless
<i>y_{CO₂}</i>	= mole fraction of CO ₂ in vapor phase, dimensionless
<i>z</i>	= unknown compressibility

Greek symbols

$\phi^L_{CO_2}$	= liquid-phase partial fugacity coefficient for CO ₂ , dimensionless
$\phi^{Sat}_{CO_2}$	= fugacity of pure CO ₂ vapor at <i>P^{Sat}_{CO₂Solid}</i> , dimensionless
$\phi^V_{CO_2}$	= vapor-phase partial fugacity coefficient for CO ₂ , dimensionless
γ_{CO_2}	= activity coefficient for CO ₂ in the liquid phase, dimensionless



■ Figure 2. Frost point and dew point isotherms for the CH_4+CO_2 binary system.

dicted triple point locus agrees well with the experimentally measured triple point locus for vapor-phase methane compositions above 90%mol.

At lower methane concentrations, errors in the predicted dew point isotherms throw off the predicted triple point isotherm. The predicted dew point isotherms were calculated with a commercial process simulator using the Peng-Robinson equation-of-state model with default values for the interaction parameters. In defense of the simulator, the dew point predictions for $y_{\text{CH}_4} < 0.9$ qualitatively agree with other experimental measurements (5, 19) not shown in Figure 2. Resolution of this discrepancy is beyond the scope of this article.

Fortunately, most practical applications operate in the right-hand side of Figure 2, in the region between the triple point and critical locus. This example, though, does show the importance of also validating vapor/liquid equilibria predictions in addition to the liquid/solid and vapor/solid predictions.

The numerical methods used to solve Eq. 4 for the conditions at which frosting occurs are basically the same as those used to solve the LSE relationship given in Eq. 2. To avoid the pitfall of an improperly evaluated fugacity, we again recommend using a conservative root-finding method, such as false position, but this time the calculation can be initialized with the result of a converged solution to Eq. 4 under the assumption of ideality (*i.e.*, the fugacities and exponential Poynting factor terms of Eq. 4 are set to unity).

Calculation procedures for unit operations

The usual approach for avoiding CO_2 freezing conditions uses thermodynamics to predict freezing temperatures at key locations within the cryogenic process. A minimum temperature safety margin is then employed to ensure that CO_2 freezing conditions are avoided. This allows for adequate operating flexibility, including off-design operation, and accounts for the uncertainty in the freeze point prediction. The temperature safety margin is defined as the temperature difference between the operating temperature and the temperature at which freezing is predicted at a particular phase composition and system pressure.

The following sections describe how the calculations can be tailored

for specific unit operations. The analysis uses thermodynamics with the bulk fluid properties to predict CO_2 freezing. There are several limitations inherent to this approach (*e.g.*, potential for boundary layer freezing, kinetics of solid CO_2 nucleation and growth, unit operations not accurately described by equilibrium thermodynamics). These issues require a more detailed analysis that is beyond the scope of this article.

Heat exchangers

Consider CO_2 freezing calculations for a fluid being cooled in the warm side of a heat exchanger. If the warm side stream is a vapor that is cooled but not condensed inside the exchanger, then only a VSE freeze calculation is required for the outlet stream. Likewise, if the warm side stream is all liquid, then only an LSE freeze calculation is required. If the warm side stream condenses within the exchanger, it is necessary to proceed step-wise through the exchanger, performing VSE and LSE freeze calculations at a suitable number of temperature/composition increments.

To illustrate the value of this approach, consider the hypothetical example represented by Figure 3. The warm feed enters as a saturated vapor (Point A). As it cools, heavier components preferentially condense, creating a varying liquid-phase composition along the exchanger pass. Since CO_2 is heavier than methane, it tends to concentrate in the liquid phase, and it is possible to reach a point at which the liquid solubility is exceeded and the CO_2 could freeze and potentially plug

the exchanger (Point B). Assume that the stream is further cooled (ignoring the CO₂ freezing potential). Eventually, enough methane will condense and the CO₂ solubility in the liquid will increase to the point where all of the CO₂ can be held in the liquid phase again without freezing (Point C). With continued cooling of this stream, full condensation occurs (Point D). Subcooling will eventually cause the liquid solubility to be exceeded again (Point E), where CO₂ could freeze again.

In this case, evaluation of only the outlet stream would lead to the correct prediction of a potential freezing problem with the exchanger. However, if the example was modified so that the warm outlet stream temperature was given as Point D, or anywhere between Points C and E, the potential freezing problem would be undetected. This pitfall can be avoided by the incremental method discussed here.

Notice that the definition of the temperature safety margin depends on the phase composition being constant. The inherent problem of the CO₂ freeze utility of at least one commercial process simulator is that it performs VLE flash calculations while searching for the nearest freeze point. The example in Figure 3 shows that multiple solutions to the freeze point problem (*i.e.*, Points B, C and E) may exist if the phase compositions are allowed to vary. This pitfall of multiple solutions can be avoided by using freeze prediction routines that do not conduct VLE flash calculations while searching for a freeze point and that are customized to the needs of the specific unit operation.

Expanders

The procedures for predicting CO₂ freeze points within expanders are similar to those used for exchangers. If no phase change occurs within the expander, then an outlet stream VSE freeze calculation is sufficient. If condensing does occur within the expander, then VSE and LSE freeze calculations are performed at incremental pressure steps.

In actual operation, expanders do not always internally obey equilibrium thermodynamics. The internal velocities can sometimes be quite high and there may not be sufficient residence time to establish vapor/liquid equilibrium at any given point other than at the outlet. Nonetheless, an incre-

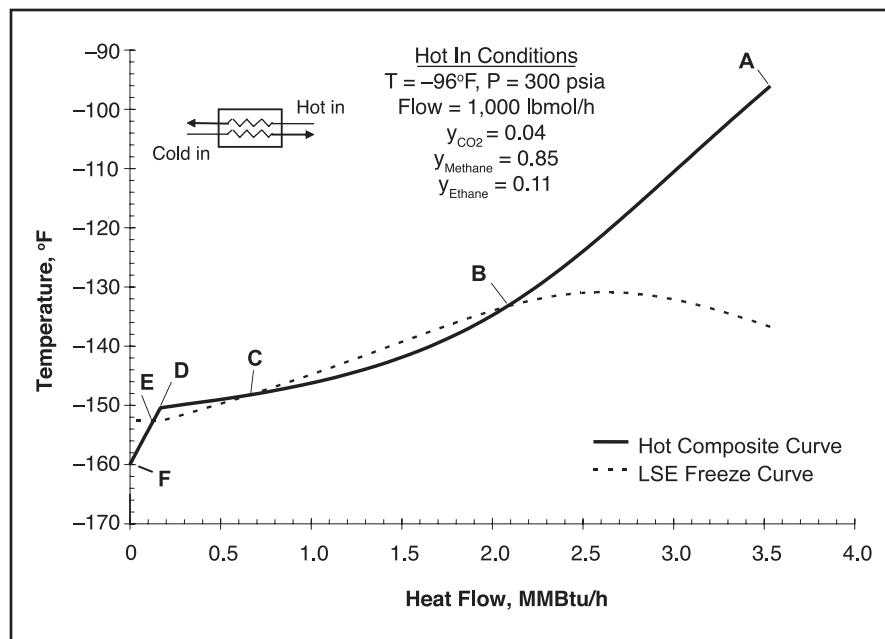


Figure 3. An exchanger profile with multiple freeze points.

mental analysis should be adequate for an initial analysis. Further assistance from an expander vendor or other experts should be enlisted for a more detailed analysis.

Columns

The methodology for CO₂ freezing prediction within columns is the same as that for any other equipment handling mixed liquid and vapor phases.

Liquid-phase CO₂ freezing calculation procedures are the same for either packed or trayed columns. For each stage in the column, the temperature safety margin is calculated by comparing the stage temperature to the CO₂ freezing temperature predicted by an LSE calculation using either Eq. 1 or Eq. 2.

Vapor-phase CO₂ freezing calculation procedures differ slightly, depending on whether a packed or a trayed column is being considered. For each stage in a packed column, the temperature safety margin is calculated by comparing the stage temperature to the CO₂ freezing temperature predicted by a VSE calculation using Eqs. 4 and 5. Vapor-phase freezing in a packed column may be mitigated by washing the solid CO₂ with the down-flowing liquid. Determining the ultimate fate for this solid CO₂, once formed, is beyond the scope of this article, which focuses on how to avoid situations in which solid will form.

The procedure for a trayed column is similar, however, the temperature safety margin for each stage is calculated by comparing the temperature of the tray above with the CO₂ freezing temperature predicted by a VSE

calculation. Recall that while the vapor is in equilibrium with its tray liquid, the vapor will contact the colder tray above. Any cooling of the vapor past its vapor/solid equilibrium point may result in desublimation of solid

CO₂ onto the cold underside surface of the tray above. Weeping, frothing, entrainment, etc. may wash the solid CO₂ off of the bottom of the tray above, but the analysis of the ultimate fate of the CO₂ and evaluating the potential for plugging in this situation are also beyond the scope of this article.

Literature Cited

1. Kurata, F., "Solubility of Solid Carbon Dioxide in Pure Light Hydrocarbons and Mixtures of Light Hydrocarbons," Research Report RR-10, Gas Processors Association, Tulsa, OK (1974).
2. Knapp, H., et al., "Solid-Liquid Equilibrium Data Collection: Binary Systems," Chemistry Data Series Vol. VIII, Part I, DECHEMA (1987).
3. Davis, J. A., et al., "Solid-Liquid-Vapor Phase Behavior of the Methane-Carbon Dioxide System," *AIChE J.*, **8** (4), pp. 537–539 (1962).
4. Brewer, J., and F. Kurata, "Freezing Points of Binary Mixtures of Methane," *AIChE J.*, **4** (3), pp. 317–318 (1958).
5. Donnelly, H. G., and D. L. Katz, "Phase Equilibria in the Carbon Dioxide-Methane System," *Ind. Eng. Chem.*, **46** (3), pp. 511–517 (1954).
6. Cheung, H., and E. H. Zander, "Solubility of Carbon Dioxide and Hydrogen Sulfide in Liquid Hydrocarbons at Cryogenic Temperatures," *Chem. Eng. Progress Symposium Series*, **64**, pp. 34–43 (1968).
7. Mraw, S. C., et al., "Vapor-Liquid Equilibrium of the CH₄-CO₂ System at Low Temperatures," *J. Chem. Eng. Data*, **23** (2), pp. 135–139 (1978).
8. Sterner, C. J., "Phase Equilibria in CO₂-Methane Systems," *Adv. Cryog. Eng.*, **6**, pp. 467–474 (1961).
9. Jensen, R. H., and F. Kurata, "Heterogeneous Phase Behavior of Solid Carbon Dioxide in Light Hydrocarbons at Cryogenic Temperatures," *AIChE J.*, **17** (2), pp. 357–364 (Mar. 1971).
10. Clark, A. M., and F. Din, "Equilibria Between Solid, Liquid and Gaseous Phases at Low Temperatures: The System Carbon Dioxide + Ethane + Ethylene," *Disc. Faraday Society*, **15**, pp. 202–207 (1953).
11. Im, U. K., and F. Kurata, "Solubility of Carbon Dioxide in Mixed Paraffinic Hydrocarbon Solvents at Cryogenic Temperatures," *J. Chem. Eng. Data*, **17** (1), pp. 68–71 (1972).
12. Din, F., "Thermodynamic Functions of Gases," Vol. 1, Butterworths, London (1962).
13. Im, U. K., "Solubility of Solid Carbon Dioxide in Certain Paraffinic Hydrocarbons: Binary, Ternary and Quaternary Systems," Ph.D. Thesis, University of Kansas (May 1970).
14. Zhi, Y., and H. Lee, "Fallibility of Analytical Roots of Cubic Equations of State in Low Temperature Region," *Fluid Phase Equilibria*, **201**, pp. 287–294 (2002).
15. Press, W. H., et al., "Numerical Recipes in FORTRAN 77: The Art of Scientific Computing," 2nd ed., Vol. 1, p. 368, Cambridge University Press (1992).
16. Poling, B. E., et al., "Thermodynamic Properties from a Cubic Equation of State: Avoiding Trivial Roots and Spurious Derivatives," *Ind. Eng. Chem. Proc. Des. Dev.*, **20** (1), pp. 127–130 (1981).
17. Pikaar, M. J., "A Study of Phase Equilibria in Hydrocarbon-CO₂ System," Ph.D. Thesis, University of London, London, England (Oct. 1959).
18. Hwang, S. C., et al., "Dew Point Study in the Vapor-Liquid Region of the Methane-Carbon Dioxide System," *J. Chem. Eng. Data*, **21** (4), pp. 493–497 (1976).
19. Neumann, A., and W. Walch, *Chemie Ingenieur Technik*, **40** (5), p. 241 (1968).

Model testing

We have implemented the thermodynamic models and calculation procedures discussed here as a custom CO₂ freeze-point-prediction utility that is an add-in to a commercial process simulator. To test the software, we checked our freeze point predictions against actual data from several operating commercial-scale cryogenic gas plant demethanizers that have established CO₂ freezing limits. Confidentiality restricts the amount of detail we can provide, but the results of the comparison are shown in Table 2. Predicted freeze temperatures agree quite well with the observed plant data.

CEP

Table 2. Comparison of actual plant freezing vs. this work.

	Plant			
	1	2	3	4
Observed Plant Freeze Temperature, °F	-150.2	-142.2	-137.5	-117.0
Predicted Freeze Temperature (This Work), °F	-145.7	-141.0	-137.1	-116.2
Absolute Difference, °F	4.5	1.2	0.4	0.8
Limiting Freezing Criteria	LSE	VSE	VSE	LSE

TIM EGGEMAN is a consulting process engineer at River City Engineering (1202 E. 23rd St., Suite B, Lawrence, KS 66046; Phone: (303) 358-6390; E-mail: teggeman@rivercityeng.com). He has 15 years of industrial experience in natural gas processing, oil refining, and renewable fuels and materials. He holds a BS in chemical engineering from the Univ. of Illinois, and MS and PhD degrees in chemical engineering from the Univ. of Kansas. He is a licensed professional engineer and a senior member of AIChE.

STEVE CHAFIN is a consulting process engineer at River City Engineering (Phone: (785) 842-9073; E-mail: schafin@rivercityeng.com). For the last nine years, he has provided consulting services for natural gas and oil production facilities, both within the U.S. and abroad. He previously worked for STRATCO, the refining alkylation technology licensor, and Vulcan Chemicals. He received a BS in chemical engineering from the Univ. of Kansas and is a senior member of AIChE.

ACKNOWLEDGMENTS

The authors wish to thank ConocoPhillips, Dan Hubbard of HPT, Inc., and Julie Howat of the Univ. of Kansas Kurata Thermodynamics Laboratory for their assistance.